ELSEVIER

Thermochimica Acta 322 (1998) 17–23

thermochimica acta

Sol–gel preparation and crystallisation of $2.5CaO{\cdot}2SiO_2$ glassy powders

G. Laudisio*, M. Catauro, A. Costantini, F. Branda

Department of Materials and Production Engineering, University of Naples Federico II, P. le Tecchio, 80125 Naples, Italy

Received 12 January 1998; accepted 12 June 1998

Abstract

$2.5CaO{\cdot}2SiO_2$ gel was synthesised by hydrolytic polycondensation of tetramethyl orthosilicate (TMOS) with calcium nitrate in alcoholic medium. Thermal treatments were carried out to convert the gel into the glass. However, a completely amorphous sample was not obtained.

The gel-derived material structure was examined by FTIR spectroscopy. The IR spectra suggested that the gel-derived material has a different structure than the corresponding melt-quenched glass, for having a more uniform distribution of non-bridging oxygens among the SiO_4 tetrahedra.

Crystallisation of the gel-derived material, examined by differential thermal analysis is reported and discussed. The activation energy for crystal growth, E_c=782 kJ/mol, and the Avrami parameter, n=1, which indicates a surface nucleation mechanism, were evaluated by non-isothermal methods.

The results were compared with those obtained for a conventionally prepared glass of the same composition. © 1998 Elsevier Science B.V.

Keywords: Calcium silicate glass; Kinetic parameters; Non-isothermal devitrification; Sol–gel synthesis

1. Introduction

The sol–gel method of making inorganic glasses has been intensively studied in recent years [1]. Interest in this process has been stimulated, in part, by the low preparation temperature. The preparation involves hydrolysis and polycondensation of organometallic compounds. A gel forms which is dried to a porous particulate material. Proper thermal treatments are, therefore, required to convert the gel into the glass.

The reported work is part of a more general study with the ultimate technological objective of determining the suitability and advantages of gels as starting materials for the preparation of bioactive glasses and glass ceramics. In a previous paper [2], glasses of composition $2CaO{\cdot}3SiO_2$ were prepared by means of the sol–gel route starting from tetramethyl orthosilicate and calcium nitrate tetrahydrate and by the melt-quenching technique from a mixture of oxides. Their structure were compared. The infrared spectra suggested that the gel-derived glass has a different structure than the corresponding melt-quenched glass, having a more uniform distribution of non-bridging oxygen among the SiO_4 tetrahedra. Owing to its porosity, the gel-derived glass appeared to be more prone to devitrify than the melt-quenched glass is. The infrared spectra relative to the sample soaked in a fluid simulating the composition of the human blood plasma suggested that, according to literature [3],

*Corresponding author. Tel.: +39-81-76823; fax:+39-81-768394.

PII: S0040-6031(98)00487-0

the gel-derived glass is more bioactive than the melt-quenched glass is. This indicates that the sol–gel method is suitable for the preparation of bioactive materials.

In this paper, the sol–gel method was applied to prepare an amorphous calcium silicate, whose composition, $2.5CaO{\cdot}2SiO_2$, is richer in calcium than that described above, and is in the composition range of bioactive glasses of the $CaO–SiO_2$ system [4]. Its crystallisation behaviour was studied with the aid of X-ray diffraction and differential thermal analysis. The selected composition was chosen because the crystallisation of the corresponding melt-quenched glass had previously been studied [5] and the results obtained for the gel-derived material could be compared with those obtained for the conventional glass.

2. Experimental

A glass of composition $2.5CaO{\cdot}2SiO_2$ was prepared by means of the sol–gel method using tetramethyl orthosilicate (TMOS) and calcium nitrate tetrahydrate analytical grade reagents as starting materials. Fig. 1 shows the flow chart of glass synthesis by the sol–gel method. An alcoholic solution of TMOS was mixed under continuous stirring with $Ca(NO_3)_2$ diluted in C_2H_5OH at room temperature. Under these conditions complete gelation occurred in one day. The gel obtained was clear and homogeneous. After gelation, the gel was held for 10 days at room temperature before beginning the heat treatments.

A glass of the same composition was also prepared by melting analytical grade reagents $CaCO_3$ and SiO_2 in a platinum crucible in an electrical oven for 4 h at

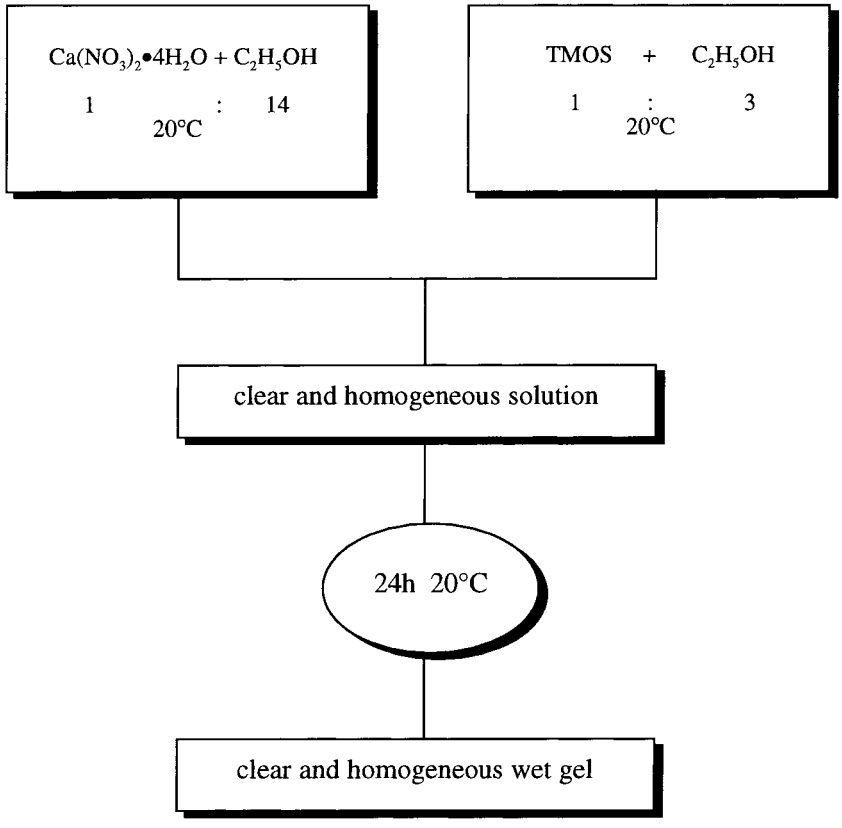

Fig. 1. Flow chart of gel synthesis.

1550°C. The melt was quenched by plunging the bottom of the crucible into cold water.

Differential thermal analysis (DTA) curves at different heating rates were recorded in air for powdered specimens of ca. 50 mg. A Netzsch heat flux DSC apparatus, model 404, was used with Al_2O_3 as reference material.

Fourier transform infrared (FTIR) transmittance spectra were recorded in the 400–1200 cm^{-1} region using a Mattson 5020 system, equipped with a DTGS KBr (Deuterated Triglycine Sulphate with potassium bromide windows) detector, with a resolution of 2 cm^{-1} (20 scans). KBr pelletised disks containing 2 mg of samples and 200 mg of KBr were made. The FTIR spectra have been elaborated by means of a Mattson software (FIRST Macros).

The amorphous nature of the gel and the devitrified samples were analysed by computer interfaced X-ray (CuK_α) powder diffractometry (XRD) using a Philips diffractometer model PW1710 with a scan speed of 1°min^{-1} and a built-in computer search program. The X-ray diffraction patterns were matched to JCPDS data and the phases identified.

3. Results and discussion

Gelation is the result of hydrolysis and condensation reactions according to the following equations:

$$Si(OCH_3)_4 + nH_2O \Rightarrow Si(OCH_3)_{4-n}(OH)_n + nCH_3OH \quad n \leq 4 \tag{1}$$

$$-SiOH + CH_3O\text{–}Si\text{–} \Rightarrow Si\text{–}O\text{–}Si\text{–} + CH_3OH \tag{2}$$

$$-Si\text{–}OH + HO\text{–}Si\text{–} \Rightarrow -Si\text{–}O\text{–}Si\text{–} + H_2O \tag{3}$$

During drying at room temperature and firing at high temperature reactions 2 and 3 go to completion and the gel shrinks to glass.

Fig. 2(a) and (b) show the DTA curves, recorded at 10°C/min, of the gel dried for 3 h at (a) 100°C and (b) of the melt-quenched glass.

As can be seen the curve of Fig. 2(a) shows three endothermic peaks in the 50–150, 450–650 temperature ranges. These peaks can be related to the evaporation of water, which can be reversibly absorbed, and alcohol, to the decomposition of nitrate [6], to completion of the hydrolysis and condensation reaction and to the consequent removal of organic compounds. The curve also shows a broad exothermic effect in the temperature range 900–950°C due to the formation of crystalline phases.

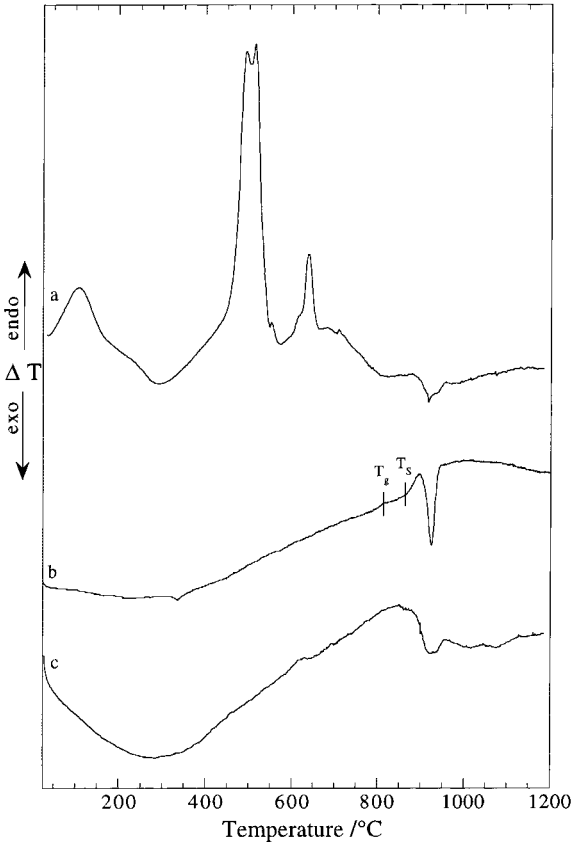

Fig. 2. DTA curves recorded at 10°C/min of: (a) gel dried for 3 h at 100°C; (b) melt-quenched glass; and (c) gel-derived materials.

Proper thermal treatments, required to convert the gel into a glassy product, were chosen taking into account the results obtained for the gel of composition $2CaO{\cdot}3SiO_2$, as described in a previous paper [2] and thermal effect shown in Fig. 2(a). The gel was slowly heated at 5°C/min till 600°C to eliminate the volatile species and the residual organic and inorganic product, and then it was rapidly heated to 790°C and kept at this temperature for 1 h. As in the case of the former paper [2], the temperature for the heat treatment was chosen relative to the glass-transformation temperature for quenched glass, taken from Fig. 2(b), T_g=810°C. Therefore, T=790°C is only 20°C lower

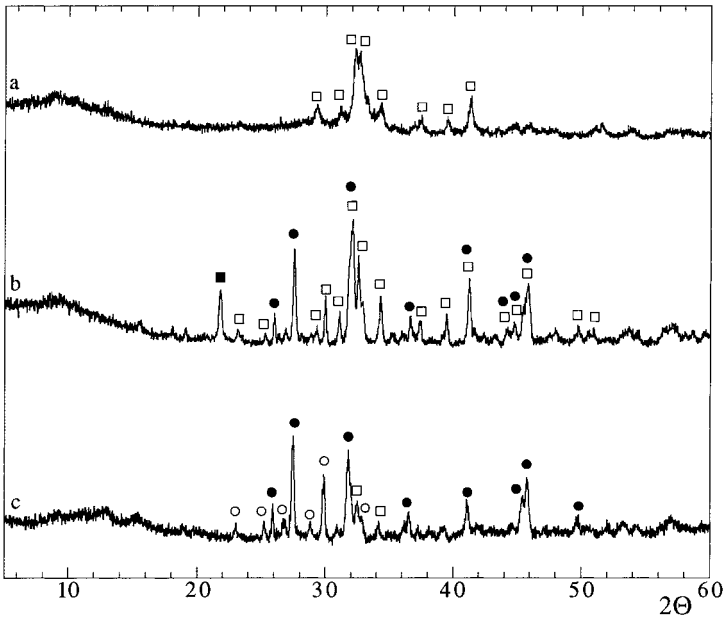

Fig. 3. X-ray diffraction patterns of: (a) gel-derived material before DTA run; (b) gel-derived material after DTA run; and (c) melt-quenched glass after DTA run. (□) alite (JCPDS card 11/593); (■) cristobalite (JCPDS card 27/605); (○) wollastonite (JCPDS card 27/88); (●) pseudowollastonite (JCPDS card 19/248).

than T_g and the gel is expected to be fluid enough for the elimination of the excess volume and reactions 2 and 3 to go to completion; otherwise it is far from the temperature range of formation of crystalline phases as shown in Fig. 2(a) and (b).

Fig. 2(c) shows the DTA curve of the gel-derived material obtained with the described heating schedule; it indicates that the devitrification occurs in the temperature range where the melt-quenched glass curve shows a slope change. This last effect can be attributed to softening of the powdered samples and to the consequent change of heat-transfer coefficient. Therefore, the gel-derived sample devitrifies in the temperature range in which the melt-quenched glass softens.

Fig. 3 shows the XRD patterns of gel-derived glass (a) before, (b) after DTA run up to 1200°C which are compared with XRD pattern of melt-quenched glass and (c) after a DTA run up to 1200°. In the gel-derived material, alite (Ca_3SiO_5) microcrystals are present as shown by the broad peaks on XRD pattern. The successful formation of glass is, in general, the result of a competition between those phenomena which lead to the densification and those which promote crystallisation. In the preparation of $2CaO{\cdot}3SiO_2$ gel-derived material, the described heat treatments [2] lead to a completely amorphous material; in the case of $2.5CaO{\cdot}2SiO_2$ composition the same heating schedule for the transformation of the gel into glass lead to the precipitation of alite microcrystals. The XRD pattern of the gel-derived material after the DTA run (Fig. 3(b)) shows several sharp reflections that were attributed to pseudowollastonite and alite. Moreover, the characteristic peak at d=4.07 of the cristobalite was also found. In the XRD pattern of the melt-quenched glass after the DTA run the peaks were attributed to wollastonite, pseudowollastonite and alite [5]. The presence of alite is consistent with a calcium amount in the mother glass higher than that in the wollastonite composition requiring the growth of calcium richer crystals. However, Fig. 3 shows that the amount of this crystalline phase in the gel-derived material is higher than in the melt-quenched glass; therefore, it is justified that the devitrification of the residual glassy matrix, richer in SiO_2 with respect to what happens in the case of melt-quenched glass, involves the formation of pseudowollastonite but also cristobalite.

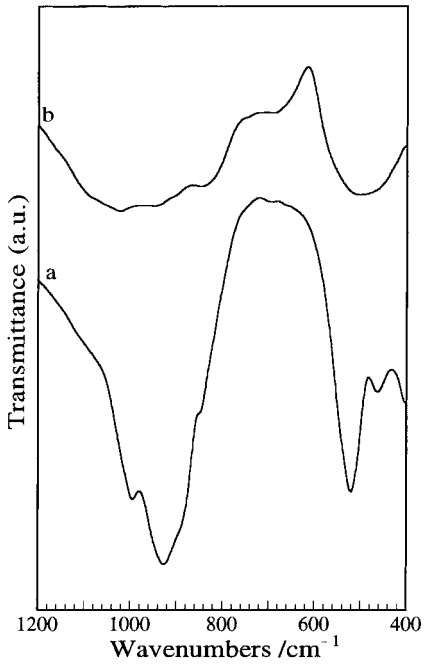

Fig. 4. Transmittance infrared spectra of: (a) gel-derived material; and (b) melt-quenched glass.

In Fig. 4(a) and (b), the infrared absorption spectra of the gel-derived material and the melt-quenched glass are respectively reported. The strong band at higher wavenumbers (800–1200 cm^{-1}) is attributed to the stretching modes of the SiO_4 tetrahedra; the band at lower wavenumbers (400–600 cm^{-1}) is attributed to the bending modes of the SiO_4 tetrahedra [7,8].

The stretching band is sharp in the gel-derived material and broad in the melt-quenched glass.

It may be recalled that the IR absorption of SiO_4, in the case of silica, is relatively sharp and occurs at 1100 cm^{-1}. When a modifier oxide is added, it shifts towards lower wavenumbers and covers a broader wavenumbers range. This has been attributed to the presence of SiO_4 tetrahedra bearing different number of non-bridging oxygen atoms [7,8]. This should give rise to a greater number of stimulated modes of vibration and can explain the shape of the band in the IR spectra of Fig. 4(b). Otherwise the absorption band of the gel-derived material is sharp and this suggests that, as already found in the case of $2CaO{\cdot}3SiO_2$ [2], the structure of the gel-derived material is characterised by a greater uniformity in the distribution of the NBOs among the SiO_4 tetrahedra with respect to the melt-quenched glass.

The devitrification behaviour of the gel-derived material was compared to that of the melt-quenched glass by means of the non-isothermal methods. The devitrification kinetic parameters were determined by using the following two equations [9–11], derived from the Johnson–Mehl–Avrami equation [12,13]:

$$\ln \beta = -\frac{E}{RT_p} + \text{const.} \quad (4)$$

$$\ln \Delta T = -\frac{nE}{RT} + \text{const.} \quad (5)$$

Eqs. (4) and (5) can also be derived, for the non-isothermal devitrification, from the following well-known equation [13,14]:

$$-\ln(1-\alpha) = (A/\beta^n)\exp(-nE/RT) \quad (6)$$

where α is the volume fraction crystallised at each temperature T, β the DTA heating rate, ΔT the deflection from the baseline at each temperature T, T_p the peak temperature and E the activation energy for the crystal growth. The Avrami parameter, n, is related to the crystallisation mechanism [13–15] (n=1, surface crystals or rod-like bulk crystals; n=2, plate-like bulk crystals; and n=3, three-dimensional bulk crystals). Eqs. (4) and (5) can be derived from Eq. (6) by assuming:

1. α at peak temperature is not dependent on the heating rate [16];
2. ΔT is proportional to the instantaneous reaction rate [17,18];
3. in the initial part of the DTA crystallisation peak the change in the temperature has a much greater effect than α on the ΔT [10].
4. the crystals grow from the same number of nuclei not dependent on the heating rate.

When plotting $\ln\beta$ against $1/T_p$ and $\ln\Delta T$ vs. $1/T$ straight lines were obtained according to Eqs. (4) and (5) (Figs. 5 and 6). Their slopes allowed, therefore, to evaluate E and nE values. The E=782 kJ/mol is slightly greater than that, E=600 kJ mol^{-1}, found for melt-quenched glass. The difference between them can be justified, however, if it is taken into account that the gel-derived material is partially devitrified and a greater activation energy is expected owing to the

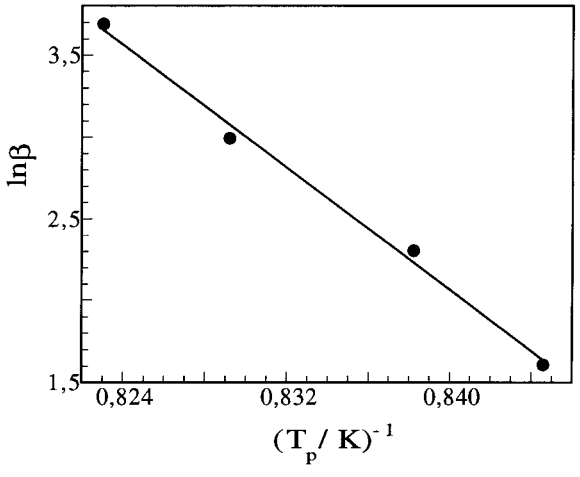

Fig. 5. Plot of $\ln\beta$ vs. $1/T_p$.

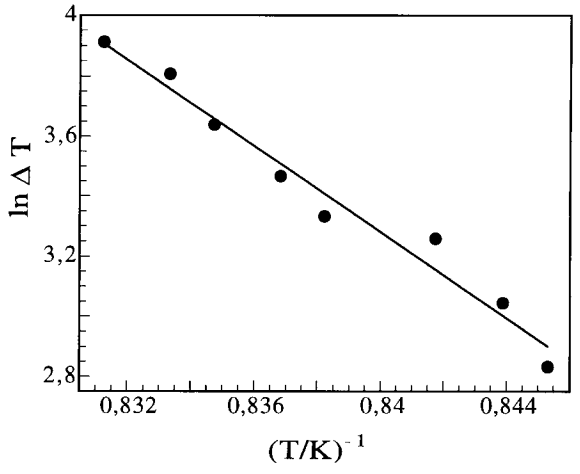

Fig. 6. Plot of $\ln\Delta T$ vs. $1/T$.

lower CaO content of the crystallising glassy matrix. The value of the Avrami parameter, $n=1$, is consistent with a surface crystallisation mechanism but differs from that of the melt-quenched glass which requires another explanation. This was explained [19] by taking into account the DTA curve recorded on fine powders of the melt-quenched glass, which shows (Fig. 2(b)), at $T>T_g$ but before the crystallisation peak, a change in slope because of the softening and consequent heat-transfer coefficient change. As a result of softening and sintering, the surface nuclei formed in the glass-transformation range become bulk nuclei and give rise to plate-like bulk crystals. This result was confirmed by SEM micrographs [19] and agrees with the results reported in the literature that wollastonite crystals are often in the form of tablets [20].

Therefore, in the case of the gel-derived material, whose DTA curve does not show the softening effect, the found value $n=1$ is as expected.

4. Conclusions

The sol–gel method was applied to prepare a glass of composition $2.5CaO{\cdot}2SiO_2$. A completely amorphous sample was not obtained owing to the presence of some amount of alite microcrystals.

The gel preparation involves hydrolysis and polycondensation of tetramethyl orthosilicate with calcium nitrate. The gel thus prepared is an amorphous solid containing water and organic residues that are lost on heating. The necessary temperatures are near the glass-transition temperature of the glass being formed, and therefore during the heat treatments required for the conversion of gel into glass, the gel is not kinetically stable to crystallisation and some amount of microcrystallites precipitates in the glassy matrix.

The IR spectra suggest that the gel-derived material has a different structure than the corresponding melt-quenched glass, for having a more uniform distribution of non-bridging oxygens among the SiO_4 tetrahedra.

Some difference, with respect to the melt-quenched glass, was also found in the XRD patterns of the fully devitrified samples obtained after a DTA run. The XRD pattern of the gel-derived materials shows the formation of lower amounts of $CaO{\cdot}SiO_2$ crystals and, consequently, greater amount of alite together with the formation of cristobalite as compared to the melt-quenched glass.

The non-isothermal devitrification was studied. The value of activation energy for crystal growth, $E=782$ kJ/mol, is slightly greater than the one, $E=640$ kJ/mol, found in the case of the melt-quenched glass. The value of the Avrami parameter, $n=1$, suggests that nuclei are preferentially formed on the sample surface; as the gel-derived material does not soften before crystallising, it devitrifies, by a surface crystallisation mechanism, on the contrary to what happens in the case of the melt-quenched glass.

References

[1] C.J. Brinker, G.W. Scherer, Sol-gel Science Academic Press 1990 Inc. San Diego, CA.
[2] M. Catauro, G. Laudisio, A. Costantini, R. Fresa, F. Branda, J. Sol-Gel Sc. Tech. 10 (1997) 231.
[3] P. Li, K. De Groot, J. Sol-Gel Sci. Tech. 2 (1994) 797.
[4] T. Kokubo, Bol. Soc. Esp. Ceram. Vid., Proc. XVI Int. Cong. Glass, Madrid, 1 (31-C1), 1992, p. 119.
[5] R. Fresa, A. Costantini, F. Branda, Termochim. Acta 302 (1997) 87.
[6] N.P. Bansal, J. Mat. Sci. 27 (1992) 2992.
[7] I. Simon, H.O. McMahon, J. Am. Ceram. Soc. 36 (1953) 160.
[8] Y. Kim, A.E. Clark, L.L. Hench, J. Non Cryst. Solids 113 (1989) 195.
[9] T. Ozawa, Polymer 12 (1971) 150.
[10] F.O. Piloyan, I.U. Ryabchikov, O.S. Novikova, Nature (London) 212 (1966) 1229.
[11] A. Marotta, A. Buri, Termochim. Acta 25 (1978) 155.
[12] W.A. Johnson, R.F. Mehl, Trans. AIME 135 (1939) 416.
[13] M. Avrami, J. Chem. Phys. 7 (1939) 1103.
[14] K. Matusita, S. Sakka, Bull. Inst. Chem. Res. Kyoto Univ. 59 (1981) 159.
[15] D.R. MacFarlane, M. Matecki, M. Poulain, J. Non-Cryst. Solids 64 (1981) 351.
[16] P.G. Boswell, J. Thermal Anal. 18 (1980) 353.
[17] H.J. Borchardt, F. Daniels, J. Am. Chem. Soc. 79 (1957) 41.
[18] K. Akita, M. Kase, J. Phys. Chem. 72 (1968) 906.
[19] F. Branda, A. Costantini, A. Buri, A. Tomasi, J. Thermal Anal. 41 (1994) 1479.
[20] A.N. Winchell, H. Winchell, The microscopical characters of artificial inorganic substances: optical properties of artificial minerals, Academic Press, New York and London, 1964, p. 291.